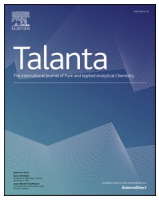
Talanta 295 (2025) 128306



Contents lists available at ScienceDirect

Talanta

journal homepage: www.elsevier.com/locate/talanta



# A novel one-tube RPA/CRISPR melting curve detection sensing system based on unique 3′-toehold nucleic acid aptamer for *Bacillus anthracis* detection

Jianhao Xu [a], Yitong Zhang [a,b], Bing Yuan [a], Yan Wang [a], Jinglin Wang [a,b,*], Yuan Yuan [a,**]

[a] State Key Laboratory of Pathogen and Biosecurity, Academy of Military Medical Sciences (AMMS), Beijing, 100071, China
[b] School of Life Sciences, Fujian Agriculture and Forestry University, Fuzhou, Fujian, 350002, China

ARTICLE INFO

*Keywords:*
CRISPR
3′-toehold nucleic acid aptamer
Melting curve
One-tube
*Bacillus anthracis* detection

ABSTRACT

Developing effective detection methods for *Bacillus anthracis* is essential for our public health system to accurately detect hidden anthrax outbreaks. Herein, we introduce a unique 3′-toehold nucleic acid aptamer (probes) into Cas12a biosensor, combined with RPA, to establish a rapid (1h), specific, and sensitive (1copy/μL) detection method for *B. anthracis*. The design behind this approach is that the target sequence is amplified via RPA, and the amplification product triggers the crRNA/Cas12a complex to degrade the 3′ toehold probes, which are analyzed using melting curve analysis on a specific instrument, naming a one-tube RPA/CRISPR melting curve detection (ORCMD) sensing system. Furthermore, ORCMD is used to detect the *B. anthracis* spores-positive or negative soil samples from the location of world War-II site (Harbin, China), *B. anthracis* was precisely identified as other methods, suggesting its significant practical application potential. This system enriches the CRISPR detection technology toolbox, compared to other CRISPR-based sensing strategies, the concept of the 3′ toehold probes offers distinct advantages in the development of CRISPR-based multi-target detection methods.

## 1. Introduction

*Bacillus anthracis*, a highly virulent pathogen, has the potential to cause anthrax in a variety of animals, including horses, cattle, sheep, and even humans [1]. Anthrax, a widely spread disease, is prevalent globally, with particular endemicity in arid and temperate regions across Eurasia, Africa, and North America [2]. In addition, *B. anthracis*, which is recognized as a potential biological weapon, has been classified by the U.S. Centers for Disease Control and Prevention (CDC) as a Class A biological warfare agent. Its misuse could seriously endanger public health and safety, potentially triggering widespread social unrest and panic [3–5].

The primary identification methods for *B. anthracis* encompass conventional microbiological techniques [6], biochemical assays [7,8], and immunological approaches [9,10], all of which are capable of effectively isolating and identifying this pathogen. However, these methods exhibit distinct shortcomings. Some are complex, time-consuming, and labor-intensive, which may impede the timely delivery of clinical treatment. Others lack sufficient specificity, rendering them susceptible to false-positive and false-negative results. Recently, CRISPR-based nucleic acid detection methods have attracted attention [11]. The literature has extensively documented the use of CRISPR/Cas12a in biosensors for in vitro diagnosis of pathogen. The signal output of these biosensors can be classified into various categories including fluorescent probes [12,13], electrochemical electrodes [14,15], lateral flow strip and enzyme-linked immunosorbent assay (ELISA) [16,17], and other modalities [18,19], each of these categories demonstrates outstanding sensitivity and specificity.

Prevailing studies have indicated that the *trans*-cleavage activity, which is activated by the Cas12a-crRNA-target DNA ternary complex, possesses remarkable select preferences for non-specific single-stranded DNA, refraining from or minimal cleaving non-specific double-stranded DNA [11,20]. However, it has been recently observed that non-specific double-stranded DNA containing a 3′ toe chain is susceptible to digestion by the ternary complex [20]. Utilizing this distinctive property, our study developed a 3′ toehold nucleic acid aptamer (probes). This 3′ toehold probes are capable of eliciting a fluorescence signal during the heating process, resulting in the generation of a distinct melting curve

* Corresponding author. State Key Laboratory of Pathogen and Biosecurity, Academy of Military Medical Sciences (AMMS), Beijing, 100071, China.
** Corresponding author.
*E-mail addresses:* wjlwjl0801@sina.com (J. Wang), miniminiyuan@163.com (Y. Yuan).

https://doi.org/10.1016/j.talanta.2025.128306
Received 1 January 2025; Received in revised form 29 April 2025; Accepted 9 May 2025
Available online 14 May 2025
0039-9140/© 2025 The Authors. Published by Elsevier B.V. This is an open access article under the CC BY-NC license (http://creativecommons.org/licenses/by-nc/4.0/).

and thus forming a characteristic peak. Furthermore, we introduced a novel one-tube RPA/CRISPR melting curve detection (ORCMD) sensing system (Fig. 1). Initially, the target sequence is amplified via RPA, and the resulting amplification product triggers the crRNA/Cas12a complex to degrade the 3′ toehold probes. Ultimately, the outcomes are visualized through melting curve analysis on the general real-time PCR instrument. Crucially, we believe that compared to other CRISPR-based sensing strategies, the innovative design of the 3′ toehold probes offers distinct advantages in the development of CRISPR-based multi-target detection methods.

## 2. Experimental section

### 2.1. Materials

*B. anthracis*, *Yersinia pestis*, *Francisella tularensis, Brucella* spp., *Burkholderia pseudomallei, Burkholderia mallei, Salmonella typhi, Vibrio cholerae, Staphylococcus aureus, Bacillus cereus, Bacillus subtilis,* and *Bacillus thuringiensis* were provided by the Institute of Microbiology and Epidemiology of the Academy of Military Medical Sciences, Beijing, China. The TwistAmp™ Basic Kit was purchased from TwistDX (Maidenhead, Berkshire, UK). The LbCas12a, RNase inhibitor and NEBuffer™ 3.1 were purchased from New England Biolabs Co (Ipswich, MA, USA). The Un1Cas12f1 (Cas14a) Nuclease and 10 × HOLMES Buffer were purchased from Tolo Biotech Co., Ltd. (Shanghai, China). All of the nucleic acid oligonucleotides used in this study were purchased from Sangong Biotech Co., Ltd. (Shanghai, China), the sequences are shown in Table S1. DNase/RNase-Free distilled, deionized water ($DDH_2O$) provided by TIANGEN Biochemical Co., Ltd (Beijing, China). SLAN-96s Real-Time PCR System produced by Shanghai Hongshi Medical Technology Co., Ltd. (Shanghai, China).

### 2.2. RPA primers, crRNA and 3′ toehold probes

Initially, the design of RPA primers, crRNA, and the two-step CRISPR reaction system was grounded in prior research conducted within our laboratory [21]. In addition, the 3′-toehold probes represent a uniquely crafted combination of fluorescent probes. Depending on the base composition and length of the target fragment, this probe can be artificially tailored to exhibit varying melting temperatures (Fig. 2A). Furthermore, a short base sequence (12 nt) protruding at the 3′ end allows the 3′-toehold probes to be non-specifically cleaved by the CRISPR ternary complex. The nucleic acid sequences of RPA primers, crRNA, and the 3′ toehold probes are presented in Table S1.

### 2.3. Establishment and optimization of reaction system

Firstly, we conducted a comparative analysis of the efficacies of the two-step, one-pot, and one-tube methods. The 3′ toehold probe was digested by two-step CRISPR method, one-tube method (CRISPR system placed on the lid) and one-pot method (RPA + CRISPR mixed) primary reaction system (Table S2). Following the reaction's completion, a melting curve analysis was conducted. Furthermore, we optimized the Concentration of Cas12a, concentration of the 3′ toehold probe, CRISPR reaction time, NEBuffer3.1 concentration, and the heating temperature of the lid. The components of 1 × NEBuffer3.1 included 100 mM NaCl, 50 mM Tris-HCl, 10 mM $MgCl_2$,100 μg/mL Recombinant Albumin.

### 2.4. The sensitivity and specificity of ORCMD

Upon optimization of conditions, the one-tube RPA/CRISPR melting curve detection (ORCMD) sensing system is summarized in Table S3. Pursuant to the system, the concentration gradient of positive recombinant plasmid was set to evaluate the sensitivity of ORCMD.

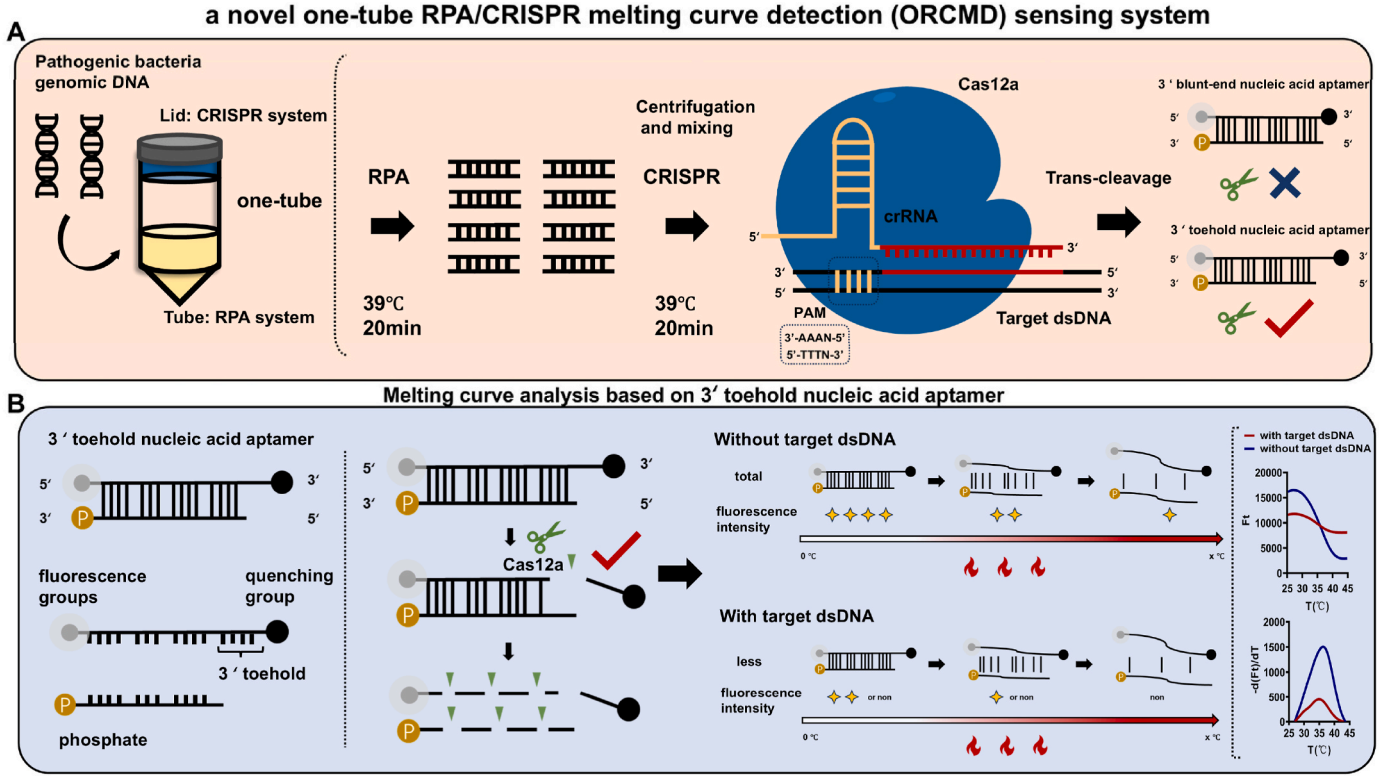



**Fig. 1.** Flowchart of the ORCMD. (A) The principle of action of 3′-toehold nucleic acid aptamer (probes), Upon the introduction of the target into the system, the activation of the *trans*-cleavage digest 3′-toehold probes initiates a reduction in the amount of fluorescence observed during the heating and melting process, potentially leading to a complete absence of fluorescence. (B) Concise overview of the operational procedure for executing the ORCMD system. Ft, fluorescent signals. T, temperature.

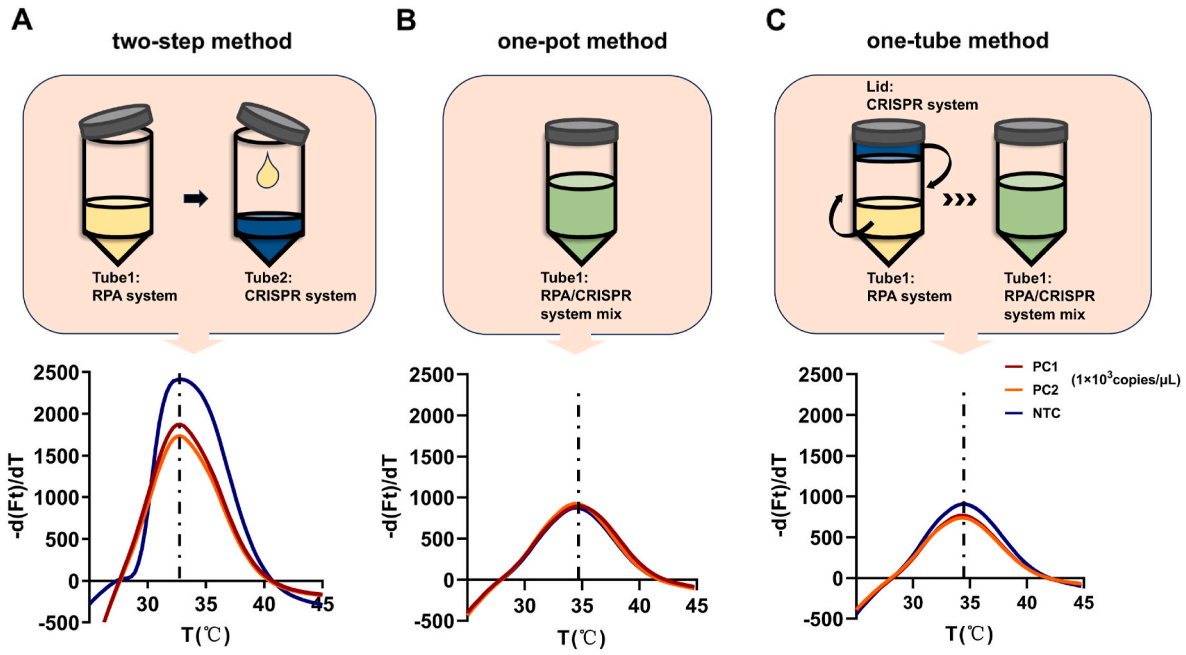



**Fig. 2.** (A), (B), (C) are the results of the two-step, one-pot, one-tube method to digest the 3′ toehold probes, respectively, n = 2.

Then, a mixed nucleic acid extract of 8 other pathogenic bacteria and 3 homologous bacteria was set to evaluate the specificity of ORCMD. Furthermore, due to the natural abundance of microorganisms and inorganic substances in anthrax samples, non-specific detection may arise. To enhance the evaluation of ORCMD's specificity, we employed nucleic acid extracts from healthy human whole blood and soil samples as negative control (samples).

### *2.5. Detection of B. anthracis in the soil samples collected from the location of world War-II site (Harbin, China) by ORCMD*

Soil samples were collected from Harbin, China in our previous research [21,22]. A total of 14 soil samples were randomly selected to assess the practical application capabilities of ORCMD. Among them, No. 3, 13, 14, 24 samples were collected at the former site of the Japanese Army Unit 731's bacterial laboratory, and No. 1–2, 2-1, 3-2, 4-2, 6-2, 7-2, 8-2, 9-2, 11-2, 12-1 samples were collected from surrounding sites in the same region. RT-PCR method [23] concurrently as a control for comparison.

## 3. Results

### *3.1. Evaluation of two-step, one-pot and one-tube reaction systems*

As depicted in Fig. 2A, B, and C, both the two-step method and the one-tube method exhibited efficient digestion of the 3′ toehold probes, yielding a more prominent positive signal. Conversely, the one-pot method did not produce a positive signal. It is noteworthy that in comparison to the two-step method, both the one-pot and the one-tube methods eliminate the need for opening the tube cap. This advantage helps prevent aerosol pollution that might arise from multiple additions to the system. Furthermore, these methods save time and enhance overall efficiency. Moreover, while the one-pot method offers significant time and step savings (No centrifugation and mixing steps required), its reaction efficacy after pre-mixing is noticeably inferior to the one-tube method. Consequently, we have prioritized optimizing the one-tube method.

### *3.2. Optimization of one-tube method*

In this study, we primarily focus on optimizing the following conditions: concentration of Cas12a, probes concentration, NEBuffer 3.1 concentration, CRISPR reaction time, and lid temperature. In addition, we incorporated a 3′ blunt-end probe devoid of the toe chain, which was concurrently reacted with 3′ toehold probes. Initially, the impact of varying Cas12a protein concentrations on reaction outcomes was assessed, revealing a most pronounced peak height difference at a concentration of 200 nM (Fig. 3B). Then, our findings revealed that the CRISPR/Cas12a system exhibits selectivity towards double-stranded DNA harboring the toe chain (Fig. 3C). As Fig. 3D illustrates, with an increasing concentration of the 3′ toehold probes, the peak of the melting curve also rises. However, once the concentration exceeds 500 nM, the peak begins to shift towards a higher melting temperature (Tm). Based on these observations, we have selected 400 nM as the optimal probes' concentration.

Furthermore, we screened for the optimal conditions by establishing concentration gradients of NEBuffer 3.1 and varying the lid heating temperature. Fig. 3E demonstrates a significant trend: as the concentration of NEBuffer 3.1 escalates up to 1.5 × and 1.75 × , the positive signal intensifies. However, a further increase in concentration, reaching 2 × , leads to a diminished positive signal. Therefore, the reaction was conducted using 1.5 × NEBuffer 3.1. Subsequently, we envisioned that an optimal lid temperature would facilitate the assembly of Cas12a and crRNA into a binary complex prior to the reaction, thus enhancing its affinity for the target. Consequently, we implemented a temperature gradient to verify our hypothesis and discovered that a superior positive signal was achieved when the lid temperature was set at 37 °C (Fig. 3F). As depicted in Fig. 3G, the positive curve exhibits a gradual flattening trend with an extended reaction time. Taking into account both the RPA amplification duration and the subsequent melting curve analysis, a CRISPR reaction time of 20 min is deemed the most appropriate.

Moreover, we incorporated the Cas14a protein, exhibiting *trans*-cleavage activity [24], and tested its interaction with both 3′-blunt-end and 3′-toehold probes. The results in Fig. S1, demonstrate that Cas14a can digest 3′-toehold probes (The peak value of positive control was significantly lower than that of negative control), suggesting the potential applicability of the ORCMD system across various CRISPR

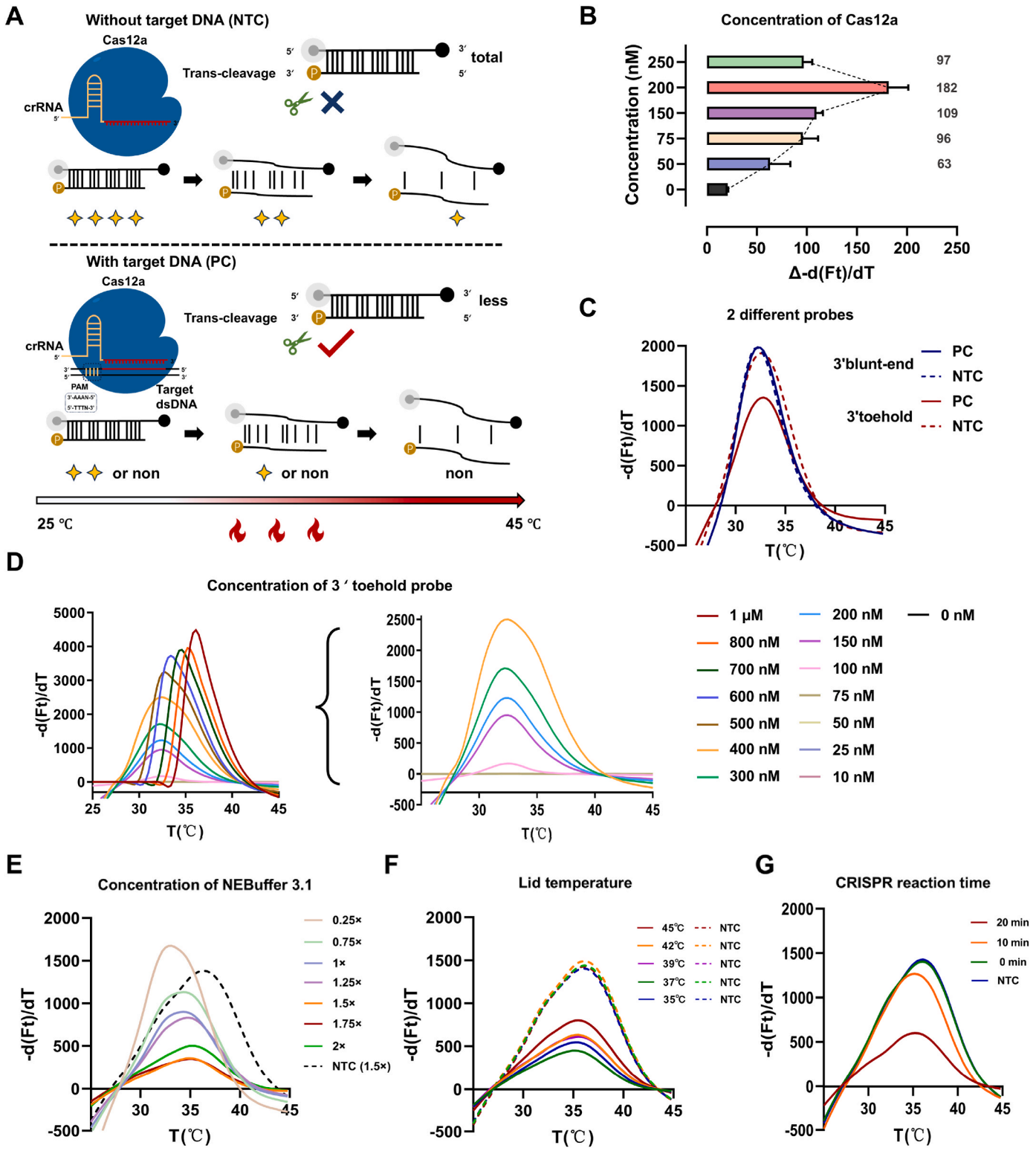



**Fig. 3.** The conditional optimization procedure of the ORCMD. (A) The principle of action of 3′-toehold probes. (B) Concentration of cas12a evaluation, n = 2. (C) Comparative experimental results of 3 ′ blunt-end and 3 ′ toehold probes. (D) Concentration of 3′ toehold probes. (E) CRISPR reaction time. (F) Concentration of NEBuffer 3.1. (G) Lid temperature.

effectors. Unexpectedly, we observed that Cas14a, unlike Cas12a, can degrade 3′-blunt-end probes. To date, this phenomenon remains unreported. This finding necessitates further exploration in subsequent studies. However, the digestion of 3′-blunt-end probes does not impact the application of the melting curve to the CRISPR/Cas14a effector, rather, it will enhance its application potential. (Fig. S1B).

### 3.3. Different 3′ -toehold probes used for multiple detection

In addition to F1–*B. anthracis*, we devised two distinct sets of 3′-toehold probes, characterized by varying melting temperatures, toe sequence and fluorescence markers, to preliminarily assess their potential for multiplex detection. The specific nucleic acid sequences are

outlined in Table S1. As shown in Figs. 4A and 3' -toehold probes F1 and F2 have the same FAM fluorescence labeling. The peak of Tm range of F1 is 34~38 °C, and the peak of Tm range of F2 is 53~57 °C. The 3' -toehold probes H1 is labeled by HEX fluorescence, and its peak of Tm range is 51~54 °C. Furthermore, H1 possesses a distinct 3′-toehold sequence from F1/F2, and the experimental outcomes reveal that the fluorescence peak is notably diminished compared to the F1/F2 probes. Therefore, we can achieve the specific detection of 10 or more targets in the future by adjusting and combining the fluorescent markers, toe sequence and Tm of 3' -toehold probes, and locking different pathogens in each combination (Fig. 4B). Preliminary validation was conducted by incorporating Cas14a to specifically target and detect the *Brucella* spp. The sequences of Cas14a-crRNA and tracrRNA are presented in Table S1. As depicted in Fig. 4C, simultaneous detection of *B. anthracis* and *Brucella* spp. was successfully achieved within a single reaction unit.

### 3.4. The sensitivity and specificity of ORCMD

To assess the sensitivity of ORCMD, we established a concentration gradient of the recombinant positive plasmid ranging from 1 to 1000 copies/μL as the positive template, while using $DDH_2O$ as the non-template control (NTC). As illustrated in Fig. 5A and B, the sensitivity of ORCMD reaches a threshold of 1 copy/μL.

In the specificity evaluation, the nucleic acid extract of *B.anthracis* (100 fg/μL), the mixed nucleic acid extract of 8 pathogenic bacteria and 3 homologous bacteria (non-*B.anthracis*, ~100 pg/μL), and the mixed nucleic acid extract of human whole blood and soil samples (>1 ng/μL) were set for simultaneous detection. As shown in Fig. 5C, ORCMD only had positive signals for the nucleic acid extracts of *B.anthracis*, had no positive signals for the nucleic acid extracts of 8 pathogenic bacteria (*Y. pestis*, *F. tularensis*, *Brucella* spp., *B. pseudomallei*, *B. mallei*, *S. typhi*, *V. cholerae*, *S. aureus*) and 3 homologous bacteria (*B. cereus*, *B. subtilis*,

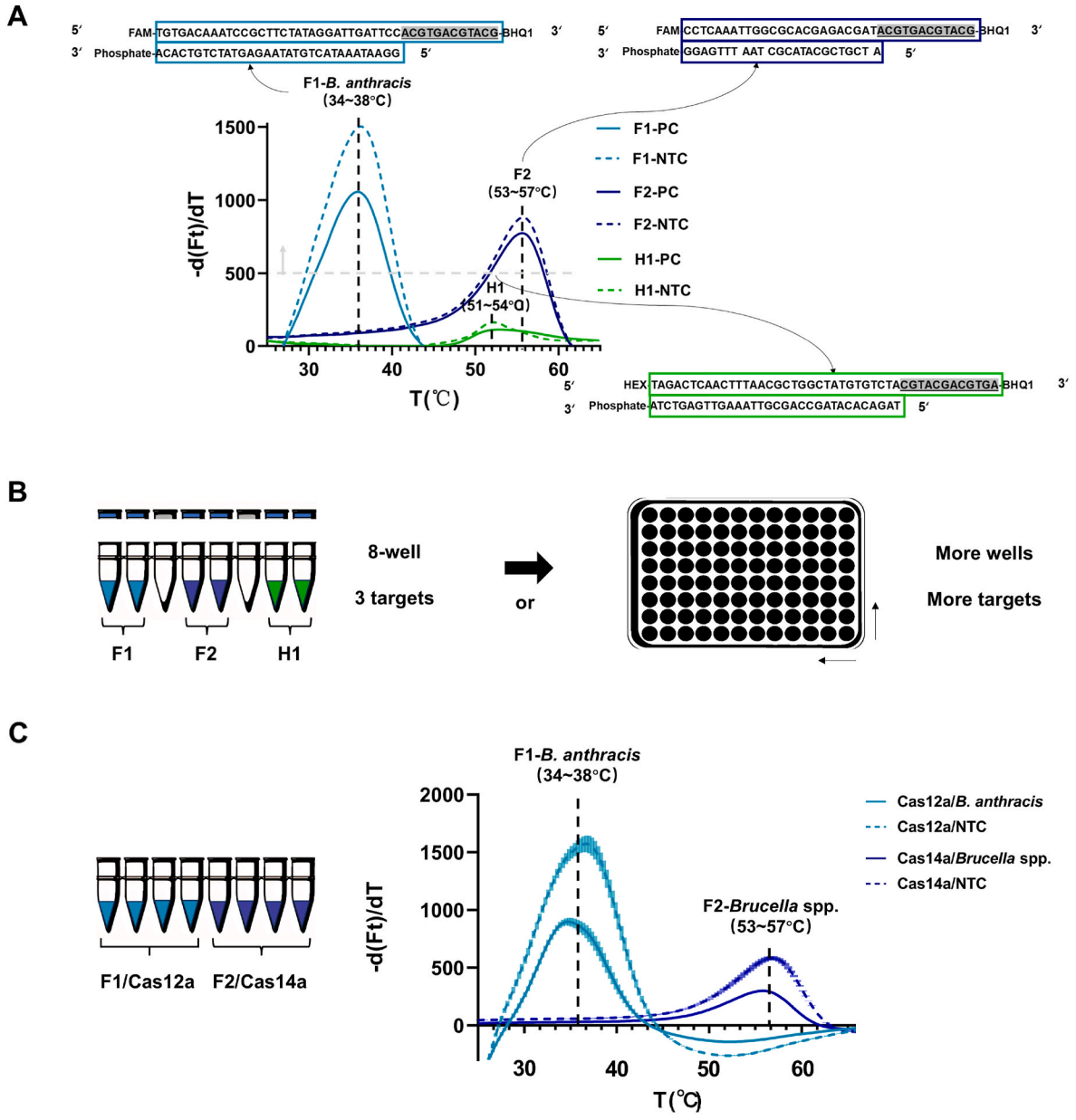



**Fig. 4.** Craft diverse 3′-toehold probes tailored for the multiplexed detection of CRISPR systems. They have different fluorescence labeling, Tm and fluorescence intensity. (A) F1, FAM, 34 °C–38 °C; F2, FAM, 53 °C–57 °C; H1, HEX, 51 °C–54 °C. (B) Expand reaction well and detection targets, and aim for screening of 10 or more pathogens in the future. (C) Actual multi-pathogen co-detection experiment, Cas12a/*Bacillus anthracis* combined with F1, Cas14a/*Brucella* spp. combined with F2, n = 2. Some of the image materials in this picture were provided by Figdraw.

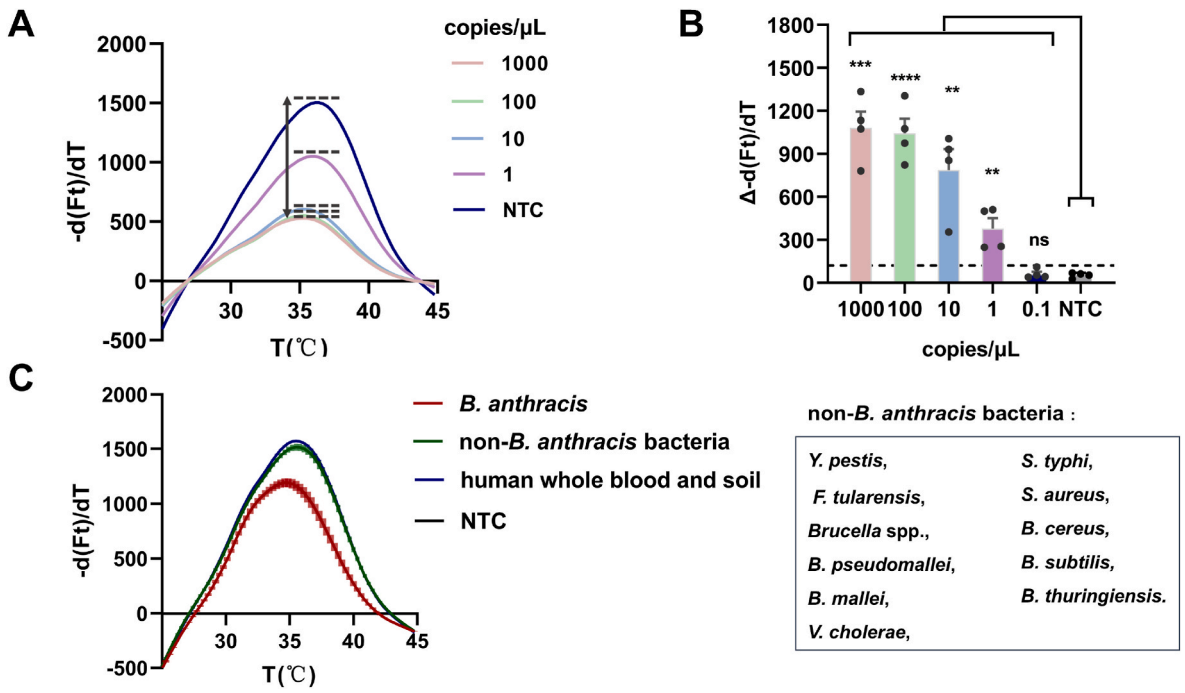



**Fig. 5.** The sensitivity and specificity of ORCMD. (A) and (B) Sensitivity evaluation of ORCMD, n = 4. The 3σ SNR values were as follows: 1000 copies/μL (SNR = 76.36), 100 copies/μL (SNR = 67.33), 10 copies/μL (SNR = 98.10), 1 copy/μL (SNR = 49.02), 0.1 copy/μL (SNR = 11.17), and NTC (SNR = 6.06). Statistical analysis was performed using a one-way ANOVA, which revealed significant differences among the groups ($p < 0.05$). The results indicate that the variations in Δ-d(Ft)/dT are statistically significant. (C) Specificity evaluation of ORCMD, n = 2.

and *B. thuringiensis*), and there was no positive signal for the nucleic acid extracts mixed with human whole blood and soil samples. The experimental results demonstrate the high sensitivity and specificity of the ORCMD developed, validating its advantages.

### 3.5. ORCMD tests actual soil samples

These samples were subjected to DNA extraction using the DNeasy PowerSoil Pro kit (Dusseldorf, Germany, QIAGEN). Briefly, 750 mg of soil and 3 mL of Solution CD1 buffer were added into a tube and boiled for 30 min in BSL-2 lab. Then, vortex briefly to mix and 800 μL of the mixture was added to the PowerBead Pro tube for extraction according to the protocol of kit. The extracted DNA was used for ORCMD analysis. The standard curve of RT-PCR has been established to quantify the target nucleic acid extracted from the sample (Fig. S2).

As depicted in Fig. 6A and B *anthracis* was positively identified in samples No. 3 and No. 24 collected within the site, with all other samples testing negative. The ORCMD and RT-PCR results were fully concordant. Subsequently, we transformed the results into an intuitive heat map and summarized the CT values of RT-PCR for clearer

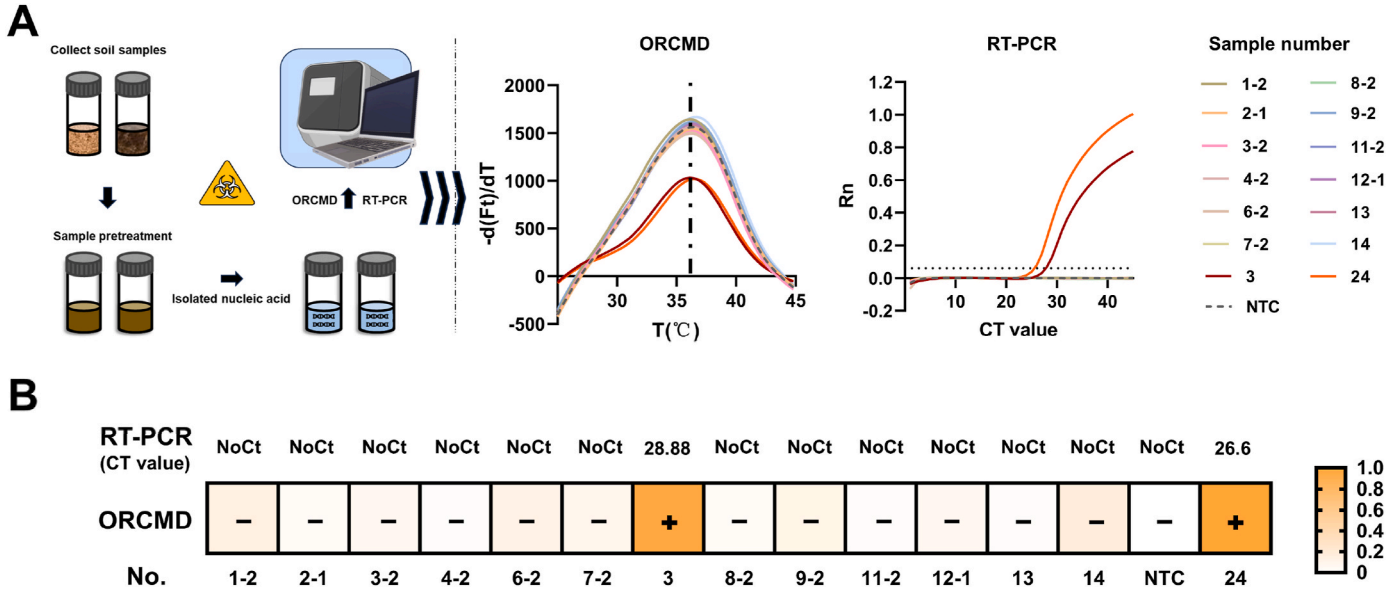



**Fig. 6.** The ORCMD system was utilized for the detection of *Bacillus anthracis* in authentic soil samples. (A) The precise coordinates of the sample collection site were recorded, along with the concurrent detection results obtained via both the RT-PCR method and the ORCMD system. (B) The results from both methods were summarized and presented in an intuitive heat map.

visualization (Fig. 6B). Furthermore, all positive samples were comprehensively validated in our prior research endeavors. The aforementioned results suggest that the ORCMD system possesses the capability to precisely detect the target pathogens in real-world environmental samples, unaffected by the nucleic acid extract of complex components, thereby demonstrating robust practical application potential.

## 4. Discussion

The development of efficient detection methods for *B. anthracis* is crucial for our public health system to efficiently screen for concealed anthrax outbreaks. Consequently, this study designed a unique 3′-toehold probes and optimized reaction conditions to establish a novel one-tube RPA/CRISPR melting curve detection (ORCMD) sensing system, enabling rapid, specific, and sensitive *B. anthracis* detection. And it can accurately detect *B. anthracis* in actual soil samples without interference from the nucleic acids of complex components within.

During the nucleic acid detection of soil samples, the accuracy of the results is frequently compromised by several interference factors [25], including chemical inhibitors (e.g., humic acids and metallic ions), physical adsorption by clay minerals, biological nucleases from coexisting microorganisms, and sample heterogeneity (humidity, pH variations, etc.). To address these challenges, several strategies are recommended: optimizing extraction reagents (e.g., EDTA for metal ions), mechanical lysis enhancement via bead-beating homogenization, physical adsorption losses may be minimized by implementing silica-based purification column optimization. It is critical to note that soil-type-specific protocol adjustments (e.g., differentiated strategies for sandy vs. clay soils). These measures can significantly enhance the efficiency of nucleic acid extraction and improve the accuracy of detection.

High-throughput and multiplexed nucleic acid detection constitutes a pivotal requirement across future molecular diagnostics, yet remains a crucial and incompletely solved necessity within the field of CRISPR/Cas biosensors [26]. In addition, different from RT-PCR, which relies on the enzymolysis of F-Q probes targeted to a specific sequence. The 'random cleavage' effect of non-specific reporter molecules due to the *trans*--cleavage activity of Cas12a, Cas12b, Cas13a, Cas14a and other Cas effector proteins, which represents a significant impediment in the development of CRISPR-based multiplex nucleic acid detection technology [27–30]. In recent years, researchers have advanced the concept of spatial multiple-detection, essentially advocating the segregation of reaction chambers for the purpose of detection of multiple pathogens in a single reaction [31,32]. These strategies effectively overcome the limitations associated with the development of CRISPR-based multiplex detection.

In this study, the 3′ toehold probes can be paired with fluorescent probes of varying excitation wavelengths, enabling a two-dimensional locking relationship between fluorescence and melting temperature. We posit that the novel 3′ toehold probes design, in contrast to other CRISPR-based sensing approaches, exhibits significant advantages in the development of CRISPR-mediated multi-target detection methods, enabling concurrent and visual identification of 10 or more targets in a single display screen (Fig. 4). This 3′ toehold probes will offer researchers an expanded array of options. Furthermore, the ORCMD system exhibits potential applicability to diverse Cas effector proteins exhibiting *trans*-cleavage capability, thereby harboring the prospect of facilitating the development of universal CRISPR-based in vitro diagnostic methodologies.

In future, to fully stimulate the potential of CRISPR as a powerful in vitro diagnostic tool, our perspective is that it is imperative to establish an amplification-free, one-tube multiplex diagnostic strategy. By eliminating the need for amplification steps, and it possesses the capability to specifically and sensitively detect a diverse range of pathogens within a single reaction system. This approach could also simplify the workflow and expedite the time to results, making it more suitable for point-of-care testing and other resource-limited settings.

## 5. Conclusion

In summary, this study developed a novel one-tube RPA/CRISPR melting curve detection sensing system, termed ORCMD, leveraging a unique 3′-toehold nucleic acid aptamer, and applied it to the detection of *B. anthracis*. The ORCMD system we have developed enriches the CRISPR detection technology toolbox, and ORCMD holds significant potential for compatibility with forthcoming high-throughput platforms, thereby facilitating the large-scale screening of highly pathogenic pathogens, bolstering public health systems' crisis response and management capabilities.

## CRediT authorship contribution statement

**Jianhao Xu:** Writing – original draft, Visualization, Validation, Software, Methodology, Formal analysis, Data curation. **Yitong Zhang:** Validation, Investigation, Formal analysis. **Bing Yuan:** Validation, Investigation, Formal analysis. **Yan Wang:** Validation, Software. **Jinglin Wang:** Supervision, Resources, Project administration, Funding acquisition. **Yuan Yuan:** Writing – review & editing, Supervision, Resources, Project administration, Funding acquisition, Conceptualization.

## Funding sources

This research did not receive any specific grant from funding agencies in the public, commercial, or not-for-profit sectors.

## Declaration of competing interest

The authors declare that they have no competing financial interests or personal relationships that could have appeared to influence the work reported in this paper.

## Acknowledgment

not applicable.

## Glossary

| | |
|---|---|
| ORCMD | one-tube RPA/CRISPR melting curve detection |
| RPA | Recombinase Polymerase Amplification |
| CRISPR | Clustered Regularly Interspaced Short Palindromic Repeats |
| RT-PCR | real time Polymerase Chain Reaction |

## Appendix A. Supplementary data

Supplementary data to this article can be found online at https://doi.org/10.1016/j.talanta.2025.128306.

## Data availability

Data will be made available on request.

## References

[1] T.C. Dixon, M. Meselson, J. Guillemin, P.C. Hanna, Anthrax, N. Engl. J. Med. 341 (1999) 815–826, https://doi.org/10.1056/nejm199909093411107.
[2] C.J. Carlson, I.T. Kracalik, N. Ross, K.A. Alexander, M.E. Hugh-Jones, M. Fegan, B. T. Elkin, T. Epp, T.K. Shury, W. Zhang, M. Bagirova, W.M. Getz, J.K. Blackburn, The global distribution of *Bacillus anthracis* and associated anthrax risk to humans, livestock and wildlife, Nat. Microbiol. 4 (2019) 1337–1343, https://doi.org/10.1038/s41564-019-0435-4.
[3] S. Liu, M. Moayeri, S.H. Leppla, Anthrax lethal and edema toxins in anthrax pathogenesis, Trends Microbiol. 22 (2014) 317–325, https://doi.org/10.1016/j.tim.2014.02.012.

[4] C.W. Hicks, D.A. Sweeney, X. Cui, Y. Li, P.Q. Eichacker, An overview of anthrax infection including the recently identified form of disease in injection drug users, Intensive Care Med. 38 (2012) 1092–1104, https://doi.org/10.1007/s00134-012-2541-0.
[5] M. Moayeri, S.H. Leppla, C. Vrentas, A.P. Pomerantsev, S. Liu, Anthrax pathogenesis, Annu. Rev. Microbiol. 69 (2015) 185–208, https://doi.org/10.1146/annurev-micro-091014-104523.
[6] T.V. Inglesby, D.A. Henderson, J.G. Bartlett, M.S. Ascher, E. Eitzen, A. M. Friedlander, J. Hauer, J. McDade, M.T. Osterholm, T. O'Toole, G. Parker, T. M. Perl, P.K. Russell, K. Tonat, Anthrax as a biological weapon: medical and public health management. Working group on civilian biodefense, J. Am. Med. Assoc. 281 (1999) 1735–1745, https://doi.org/10.1001/jama.281.18.1735.
[7] L.W. Baillie, M.N. Jones, P.C. Turnbull, R.J. Manchee, Evaluation of the biolog system for the identification of *Bacillus anthracis*, Lett. Appl. Microbiol. 20 (1995) 209–211, https://doi.org/10.1111/j.1472-765x.1995.tb00429.x.
[8] P. Lasch, W. Beyer, H. Nattermann, M. Stammler, E. Siegbrecht, R. Grunow, D. Naumann, Identification of *Bacillus anthracis* by using matrix-assisted laser desorption ionization-time of flight mass spectrometry and artificial neural networks, Appl. Environ. Microbiol. 75 (2009) 7229–7242, https://doi.org/10.1128/AEM.00857-09.
[9] D.B. Wang, B. Tian, Z.P. Zhang, J.Y. Deng, Z.Q. Cui, R.F. Yang, X.Y. Wang, H. P. Wei, X.E. Zhang, Rapid detection of *Bacillus anthracis* spores using a super-paramagnetic lateral-flow immunological detection system, Biosens. Bioelectron. 42 (2013) 661–667, https://doi.org/10.1016/j.bios.2012.10.088.
[10] A. Kuehn, P. Kovac, R. Saksena, N. Bannert, S.R. Klee, H. Ranisch, R. Grunow, Development of antibodies against anthrose tetrasaccharide for specific detection of *Bacillus anthracis* spores, Clin. Vaccine Immunol. 16 (2009) 1728–1737, https://doi.org/10.1128/CVI.00235-09.
[11] Y. Li, S.Y. Li, J. Wang, G.Z. Liu, CRISPR/cas systems towards next-generation biosensing, trends, Biotechnol. 37 (2019) 730–743, https://doi.org/10.1016/j.tibtech.2018.12.005.
[12] H.R. Cao, K. Mao, F. Ran, P.Q. Xu, Y.R. Zhao, X.Y. Zhang, H.R. Zhou, Z.G. Yang, H. Zhang, G.B. Jiang, Paper device combining CRISPR/Cas12a and reverse-transcription loop-mediated isothermal amplification for SARS-CoV-2 detection in wastewater, Environ. Sci. Technol. 56 (2022) 13245–13253, https://doi.org/10.1021/acs.est.2c04727.
[13] Y.Q. Guo, Y.F. Zhou, H. Duan, D.R. Xu, M. Wei, Y.H. Wu, Y. Xiong, X.R. Chen, S. Y. Wang, D.F. Liu, X.L. Huang, H.B. Xin, Y.H. Xiong, B.Z. Tang, CRISPR/Cas-mediated "one to more" lighting-up nucleic acid detection using aggregation-induced emission luminogens, Nat. Commun. 15 (2024) 8560, https://doi.org/10.1038/s41467-024-52931-0.
[14] F. Li, Q.H. Ye, M.T. Chen, B.Q. Zhou, J.M. Zhang, R. Pang, L. Xue, J. Wang, H. Y. Zeng, S. Wu, Y.X. Zhang, Y. Ding, Q.P. Wu, An ultrasensitive CRISPR/Cas12a based electrochemical biosensor for *Listeria monocytogenes* detection, Biosens. Bioelectron. 179 (2021) 113073, https://doi.org/10.1016/j.bios.2021.113073.
[15] M. Qing, S.L. Chen, Z. Sun, Y. Fan, H.Q. Luo, N.B. Li, Universal and programmable rolling circle amplification-CRISPR/Cas12a-mediated immobilization-free electrochemical biosensor, Anal. Chem. 93 (2021) 7499–7507, https://doi.org/10.1021/acs.analchem.1c00805.
[16] H. Li, M.L. Li, Y.C. Yang, F. Wang, F. Wang, C. Li, Aptamer-linked CRISPR/Cas12a-based immunoassay, Anal. Chem. 93 (2021) 3209–3216, https://doi.org/10.1021/acs.analchem.0c04687.
[17] Y.L. Kang, G.X. Su, Y.Y. Yu, J.J. Cao, J.L. Wang, B. Yan, CRISPR-Cas12a-based aptasensor for on-site and highly sensitive detection of microcystin-lr in freshwater, Environ. Sci. Technol. 56 (2022) 4101–4110, https://doi.org/10.1021/acs.est.1c06733.
[18] R.J. Zhao, Y.D. Tang, D.F. Song, M. Liu, B.L. Li, CRISPR/Cas12a-Responsive hydrogels for conjugation-free and universal indicator release in colorimetric detection, Anal. Chem. 95 (2023) 18522–18529, https://doi.org/10.1021/acs.analchem.3c03900.
[19] S.Q. Feng, H.J. Chen, Z. Hu, T.T. Wu, Z.H. Liu, Ultrasensitive detection of miRNA via CRISPR/Cas12a coupled with strand displacement amplification reaction, ACS Appl. Mater. Interfaces 15 (2023) 28933–28940, https://doi.org/10.1021/acsami.3c03399.
[20] N. Mohammad, L. Talton, Z. Hetzler, M. Gongireddy, Q.S. Wei, Unidirectional trans-cleaving behavior of CRISPR-Cas12a unlocks for an ultrasensitive assay using hybrid DNA reporters containing a 3′ toehold, Nucleic Acids Res. 51 (2023) 9894–9904, https://doi.org/10.1093/nar/gkad715.
[21] J.H. Xu, X.R. Bai, X.L.L. Zhang, B. Yuan, L. Lin, Y. Guo, Y.J. Cui, J.X. Liu, H.Y. Cui, X.G. Ren, J.L. Wang, Y. Yuan, Development and application of DETECTR-based rapid detection for pathogenic *Bacillus anthracis*, Anal. Chim. Acta 1247 (2023) 340891, https://doi.org/10.1016/j.aca.2023.340891.
[22] Y.R. Wu, Y. Yuan, B. Yuan, J.X. Li, J.L. Wang, Y.J. Cui, Bacteriologic and genomic investigation of *Bacillus anthracis* isolated from World War II site, China, Emerg. Infect. Dis. 30 (2024) 2687–2689, https://doi.org/10.3201/eid3012.231520.
[23] P. Cieślik, J. Knap, M. Kolodziej, T. Mirski, J. Joniec, G. Graniak, D. Zakowska, I. Winnicka, A. Bielawska-Drózd, Real-Time PCR identification of unique *Bacillus anthracis* sequences, Folia. Biol. 61 (2015) 178–183, https://doi.org/10.14712/fb2015061050178.
[24] L.B. Harrington, D. Burstein, J.S. Chen, D. Paez-Espino, E. Ma, I.P. Witte, J. C. Cofsky, N.C. Kyrpides, J.F. Banfield, J.A. Doudna, Programmed DNA destruction by miniature CRISPR-Cas14 enzymes, Science 362 (2018) 839–842, https://doi.org/10.1126/science.aav4294.
[25] U. Wydro, Soil microbiome study based on dna extraction: a review, Water 14 (2022) 3999, https://doi.org/10.3390/w14243999.
[26] Y.H. Roh, C.Y. Lee, S. Lee, H. Kim, A. Ly, C.M. Castro, J. Cheon, J.H. Lee, H. Lee, CRISPR-enhanced hydrogel microparticles for multiplexed detection of nucleic acids, Adv. Sci. 10 (2023) e2206872, https://doi.org/10.1002/advs.202206872.
[27] T. Tian, Z.Q. Qiu, Y.Z. Jiang, D.B. Zhu, X.M. Zhou, Exploiting the orthogonal CRISPR-Cas12a/Cas13a trans-cleavage for dual-gene virus detection using a handheld device, Biosens. Bioelectron. 196 (2022) 113701, https://doi.org/10.1016/j.bios.2021.113701.
[28] J.Y. Fu, L.H. Zhang, Y.L. Long, Z.H. Liu, G. Meng, H.M. Zhao, X. Su, S.B. Shi, Multiplexed CRISPR-based nucleic acid detection using a single cas protein, Anal. Chem. 95 (2023) 16089–16097, https://doi.org/10.1021/acs.analchem.3c01861.
[29] K.F. Lin, K.H. Yao, X. Li, Q.H. Li, X.J. Guo, W.X. You, W.J. Ren, Y. Bian, J.G. Guo, Z. Sun, R. Zhang, X.Q. Yang, Z.Y. Li, B.A. Li, Rapid and sensitive detection of nucleic acids using an RAA-CRISPR/Cas12b one-pot detection assay (Rcod), Talanta 271 (2024) 125616, https://doi.org/10.1016/j.talanta.2023.125616.
[30] Y.D. Wei, Z.Q. Yang, C.L. Zong, B.H. Wang, X.L. Ge, X. Tan, X. Liu, Z.Z. Tao, P. Wang, C.X. Ma, Y. Wan, J.H. Li, Trans single-stranded DNA cleavage via CRISPR/Cas14a1 activated by target RNA without destruction, Angew Chem. Int. Ed. Engl. 60 (2021) 24241–24247, https://doi.org/10.1002/anie.202110384.
[31] R.B. Peng, Z.C. Lu, M. Liu, F. Hu, RT-RPA-assisted CRISPR/Cas12a for rapid and multiplex detection of respiratory infectious viruses based on centrifugal microfluidics, Sensor. Actuat. B-Chem. 399 (2024) 15, https://doi.org/10.1016/j.snb.2023.134838.
[32] L.L. Hao, R.T. Zhao, N.L. Welch, E.K.W. Tan, Q. Zhong, N.S. Harzallah, C. Ngambenjawong, H. Ko, H.E. Fleming, P.C. Sabeti, S.N. Bhatia, CRISPR-Cas-amplified urinary biomarkers for multiplexed and portable cancer diagnostics, Nat. Nanotechnol. 18 (2023) 798–807, https://doi.org/10.1038/s41565-023-01372-9.